International Journal of Horticultural Science and Technology
Journal homepage: https://ijhst.ut.ac.ir

Green Synthesis and Characterization of Silver Nanoparticles using Feverfew (*Tanacetum parthenium* L.) Leaf and Flower Extracts

Somayeh Sadeqifard[1], Majid Azizi[1]*, Mahmoud Shoor[1], Nasrin Moshtaghi[2], Sharareh Rezaeian[3]

1 Department of Horticultural Science and Landscape Engineering, Faculty of Agriculture, Ferdowsi University of Mashhad, Mashhad, Iran
2 Department of Crop Biotechnology and Breeding, Faculty of Agriculture, Ferdowsi University of Mashhad, Mashhad, Iran
3 Industrial Fungi Biotechnology Research Department, Research Institute for Industrial Biotechnology, Academic Center for Education, Culture and Research (ACECR), Mashhad, Iran

*Corresponding author's email: azizi@um.ac.ir

ARTICLE INFO

Article history:

Received: 28 November 2024,
Received in revised form: 11 March 2025,
Accepted: 19 April 2025,

Article type:

Research paper

Keywords:

AgNPs
Nanotechnology
UV/Vis spectroscopy
Zeta potential

ABSTRACT

In recent years, science and industry have increasingly focused on nanotechnology, particularly the synthesis of nanoparticles. Although various synthesis methods are available, many are inefficient in terms of material and energy consumption. Green chemistry offers an alternative, emphasizing the use of plant-based materials as a reliable, straightforward, non-toxic, and eco-friendly approach that bridges nanotechnology and biotechnology. The present study investigated a novel method for synthesizing silver nanoparticles (AgNPs) using leaf and flower extracts of feverfew (*Tanacetum parthenium* L.). When the extract was exposed to aqueous silver ions, reduction occurred, resulting in the green synthesis of AgNPs. Ultraviolet–visible spectroscopy (UV–vis) showed a characteristic absorbance peak at 400 nm, confirming nanoparticle formation. The zeta potential of the AgNPs ranged from –30 to –90 mV, indicating good stability. Dynamic light scattering (DLS) revealed an average particle size of 68.6 nm, while field emission scanning electron microscopy (FESEM) images indicated an average size of 65.7 nm. Energy-dispersive X-ray analysis (EDX) confirmed the presence of elemental silver, validating nanoparticle synthesis. X-ray diffraction (XRD) analysis further supported these findings, showing an average particle size of 67.7 nm. Fourier-transform infrared (FTIR) spectroscopy identified peaks at 3436, 2929, 1604, 1383, and 1029 cm^{-1}, corresponding to functional groups involved in nanoparticle stabilization. In conclusion, these findings demonstrated that the nanophytosynthesis of AgNPs using *T. parthenium* extracts is a rapid, efficient, eco-friendly, and simple alternative to conventional synthetic methods.

Abbreviation: Silver nanoparticles (AgNPs), Dynamic light scattering (DLS), Energy dispersive X-ray analysis (EDX), Field emission scanning electron microscopy (FESEM), Fourier transform infrared (FTIR), Ultraviolet spectroscopy (UV-vis), X-ray diffraction (XRD)

Introduction

Nanotechnology is rapidly advancing as an interdisciplinary field with significant contributions to research, development, and industrial applications (Valle-Orta et al., 2008; Samadi et al., 2021). In recent years, nanoparticles have drawn considerable attention in modern materials science due to their unique distribution, size, and morphology (Farshchi et al., 2018; Yaqoob et al., 2020; Khan et al., 2022). Among nanomaterials, metal nanoparticles stand out for their wide range of applications in fields such as

drug delivery, magnetism, electronics, optoelectronics, agriculture, and information storage (Cui and Lieber, 2001; Bhumkar et al., 2007; Tuutijärvi et al., 2009; Zhang et al., 2010; Shahhoseini et al., 2020).

Silver nanoparticles (AgNPs), in particular, have attracted growing interest over the past two decades due to their broad utility across diverse disciplines (Srikanth et al., 2001). Metal nanoparticles with specific dimensions and morphologies can be synthesized relatively easily using chemical and physical methods (Sun et al., 2003; Alqudami and Annapoorni, 2007). However, AgNPs are especially important in biology and medicine because of their unique physical and chemical properties (Sondi and Salopek-Sondi, 2004). Silver is well known for its antimicrobial activity against a wide range of microorganisms (He et al., 2012), and in recent years, AgNPs have emerged as promising antimicrobial agents (Kaviya et al., 2011; Aziz et al., 2018). Beyond antimicrobial properties, AgNPs also exhibit antiviral, anti-inflammatory, anti-platelet, and anti-angiogenic activities, as well as cytotoxicity against cancer cells, making them highly valuable for biomedical applications (Elumalai et al., 2010; Kalishwaralal et al., 2010).

Green synthesis of AgNPs has become one of the most dynamic areas within nanotechnology (Shankar et al., 2004a). Biosynthesis of nanoparticles using enzymes (Schneidewind et al., 2012), microorganisms (Narayanan and Sakthivel, 2010), and plant extracts (Sulaiman et al., 2013; Vimalanathan et al., 2013) offers several advantages over traditional physical and chemical approaches. These methods are cost-effective, environmentally friendly, and readily scalable (Vimalanathan et al., 2013). Moreover, they eliminate the need for high temperatures, toxic chemicals, and high-pressure conditions, thereby expanding their potential medical applications (Kouvaris et al., 2012). Among biosynthetic approaches, biological reduction is a fundamental process widely applied in nano-biotechnology (El-Sayed, 2001).

Due to concerns over high energy requirements (Horwat et al., 2011), toxic byproducts (Hoag et al., 2009), and the complexity of equipment and synthesis conditions (Baruwati et al., 2009), green synthesis methods are increasingly replacing conventional techniques. Their eco-friendly nature, economic viability, and potential for large-scale production make them a promising strategy for developing advanced nanomaterials (Kouvaris et al., 2012).

Recently, plant extracts have been recognized as rich sources of bioactive constituents capable of reducing metal ions and stabilizing nanoparticles. Researchers worldwide are therefore focusing on biomolecules in plant extracts to control the size, shape, and stability of synthesized nanoparticles (Kumar and Yadav, 2009). Several plant species have already been studied for AgNPs biosynthesis, including *Magnolia kobus* and *Diospyros kaki* (Song et al., 2009a), *Gliricidia sepium* (Vilchis-Nestor et al., 2008; Rajesh et al., 2009), *Geranium* (Shankar et al., 2003), *Sorbus aucuparia* (Dubey et al., 2010), *Acalypha indica* (Kalishwaralal et al., 2010), *Coriandrum sativum* (Sathyavathi et al., 2010), *Cinnamomum camphora* (Huang et al., 2007; Yang et al., 2010), *Azadirachta indica* (Neem) (Shankar et al., 2004a), and *Aloe vera* (Chandran et al., 2006).

Tanacetum parthenium L. belongs to the Asteraceae family and is a perennial medicinal plant (Dobelis, 1986). The name of this plant is derived from the Latin word febrifugia, which means reducing fever (Rajesh et al., 2009). In the first century, the Greek physician Discorides prescribed this herb to treat "all hot inflammations" (JE). The active compounds in feverfew consist of terpenoids, flavonoids, and sesquiterpene lactones, with parthenolide being the most significant. Parthenolide (sesquiterpene lactone) with quercetin and luteolin (flavonoids) account up to 85% of the whole sesquiterpene contents in this plant. Due to its active ingredients, it possesses pain-relieving and anti-inflammatory features, making it a famous remedy for migraines and other types of headaches (Heptinstall et al., 1992). As far as we know, there is no report on the synthesis of AgNPs using feverfew leaf and flower extracts. Therefore, this study aims to explore the potential of this extract in synthesizing AgNPs while evaluating its properties for various applications.

Materials and Methods

Preparation of feverfew extract

Fresh flowers and leaves of feverfew were collected in spring from the experimental farm of Ferdowsi University of Mashhad, Iran. The plant material was thoroughly washed and shade-dried for 10 days. For extraction, 100 g of dried material was powdered and mixed with 500 mL of distilled water, followed by extraction at 40 °C using a rotary evaporator (Heidolph, Schwabach, Germany). The resulting extract was filtered to remove plant residues (Araghi et al., 2019) and stored in a cool, dark place to preserve its bioactive compounds. This method is widely recognized for producing high-quality herbal extracts while maintaining the plant's beneficial properties.

Synthesis of AgNPs

A 0.001 M aqueous solution of silver nitrate was prepared in an Erlenmeyer flask. To this, 5, 10, or 20 mL of feverfew extract was added separately, and the total volume was adjusted to 100 mL with distilled water at room temperature (Figure 1). The flasks were covered with aluminum foil and stirred continuously for 10 min. Rapid bioreduction of silver

ions occurred, indicated by a visible color change to brownish-yellow, confirming AgNP formation. After 24 h, the nanoparticle suspension was centrifuged at 15,000 rpm for 10 min (Z-326 K, Hermle Labortechnik GmbH, Germany), and the pellets were dried in a vacuum oven at 60 °C for 24 h (Balashanmugam, 2015). The purified AgNPs were collected and stored in clean bottles for subsequent characterization.

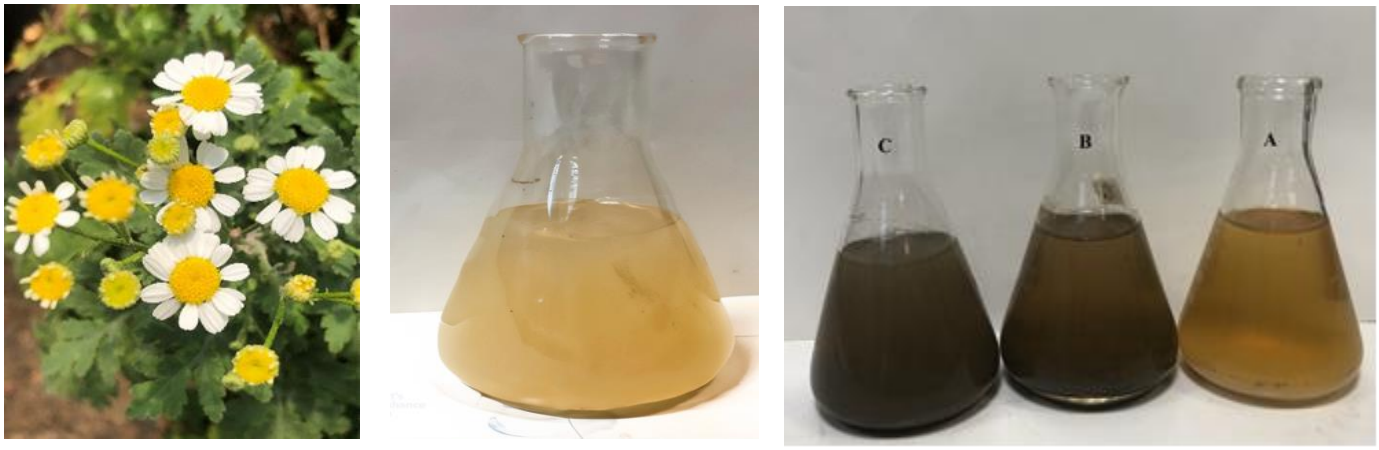

a b c

Fig. 1. (**a**) Photograph of *T. parthenium* leaf and flower; (**b**) Blend of *T. parthenium* extract and silver nitrate immediately after mixing; (**c**) Synthesized silver nanoparticles (AgNPs) after 24 h (A, B, and C indicate 5, 10, and 20 mL of feverfew extract with 95, 90 and 80 mL of 0.001 M silver nitrate aqueous solution, respectively).

UV-visible spectral analysis

The synthesis of AgNPs was confirmed by sampling the aqueous component at different time points (Song et al., 2009b; Aziz et al., 2018). The maximum absorption was then scanned using an Epoch microplate spectrophotometer (BIOTEK, USA) within the wavelength range of 300-700 nm.

Zeta potential distributions

Zeta potential gives information about the surface charge and stability of nanoparticles. This potential is an important parameter in the design of nanoparticles for various applications. Zeta potential values were measured by busing Nanopartica (HORIBA). The measurements were conducted at a temperature of 25 °C in deionized water.

Dynamic light scattering (DLS) analysis

DLS is a widely used method for measuring particle size in solutions. When a monochromatic light beam, such as a laser, is directed at spherical particles undergoing Brownian motion, a Doppler shift occurs as the light interacts with the moving particles, altering the wavelength of the incident light. This shift is directly related to particle size. Using DLS, it is possible to calculate the distribution of particle sizes and characterize particle dynamics in the medium by determining the diffusion coefficient through the autocorrelation function.

Field emission scanning electron microscopy and energy dispersive X-ray analysis

The morphology of AgNPs was examined using a ZEISS SUPRA 55 Field Emission Scanning Electron Microscope (FESEM). The images showed a uniform distribution of nanoparticles with no significant agglomeration, indicating good stability of the synthesized AgNPs. High-resolution imaging further revealed surface irregularities and nanoscale features, which may enhance the reactivity and functional performance of the nanoparticles in various applications. Elemental composition was investigated using Energy Dispersive X-ray (EDX) analysis coupled with FESEM. Elemental mapping confirmed the distribution of elements within the sample, providing valuable insights into its composition and uniformity. Overall, the combined FESEM–EDX analysis verified both the morphology and elemental makeup of the synthesized AgNPs.

X-ray diffraction studies

X-ray diffraction analysis was performed on drop-coated AgNPs films to detect the presence of Ag nanoparticles. The analysis was conducted using an X-ray diffractometer Bruker B8-advance at 40 kV voltage and 30 mA current (Unisantis XMD-300, Swiss). Diffraction intensities were recorded over 2θ angles spanning from 10° to 80°. The diffraction pattern was produced utilizing Cu-Kα1 radiation

with a wavelength of 1.5418 A° in the 2θ range of 10º to 80º at a rate of 0.02º min^{-1}, with a 2s time constant.

Fourier transform infrared spectroscopy analysis

Further evaluations using FT-IR spectroscopy were conducted to identify potential biomolecules generating silver cations (Ag^+) and to examine the coating of reduced AgNPs produced by the feverfew extract. The silver nitrate powder was obtained after centrifugation (10,000 rpm) for 15 min. Subsequently, the resultant pellet was dispersed in sterile double distilled water thrice to eliminate non-specific biological impurities such as free amino acids and proteins/enzymes that had not bound to the AgNPs ligand. Finally, the obtained AgNPs were gathered, oven-dried at 60 °C, milled with KBr pellets, and analyzed using an AVATAR 330 FTIR spectrometer in wide reproduction mode with a resolution of 4 cm x1.

Results

UV-visible spectroscopy analysis

UV/Vis spectroscopy is an effective technique for confirming both the stability and structure of AgNPs. The synthesis of AgNPs was validated by assessing two parameters: (1) changes in solution color and (2) the UV/Vis spectrum of the reaction medium. Upon adding feverfew extract to an aqueous solution of $AgNO_3$ at 60 °C, the color gradually changed from yellowish to brownish. The UV–vis spectra of AgNP solutions prepared with varying extract amounts (samples A, B, and C) are shown in Figure 2, with the inset highlighting color changes and corresponding shifts in SPR relative to extract concentration. For samples A, B, and C, the absorption peaks were primarily observed between 400–440 nm, with distinct surface plasmon resonance peaks at 416, 407, and 400 nm, respectively. Based on these results, sample C was selected for subsequent confirmation tests of AgNP synthesis.

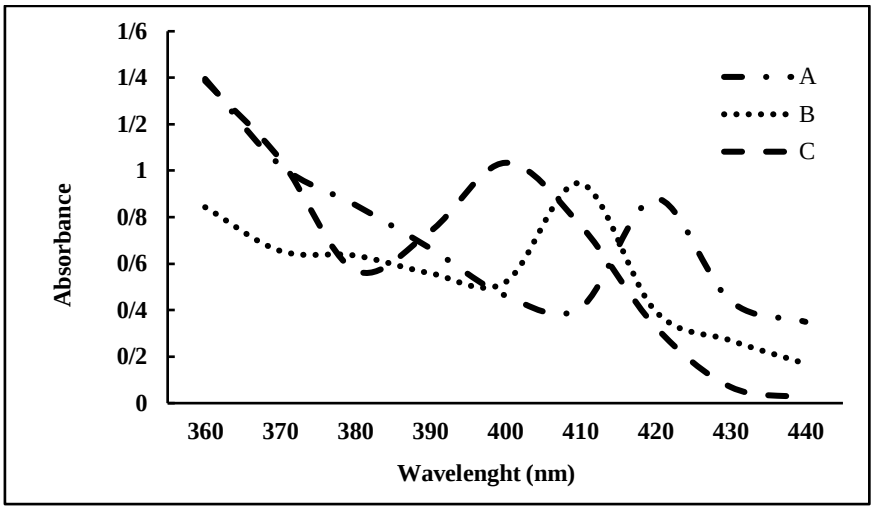

Fig. 2. UV–visible absorbance spectrum of silver nanoparticles (AgNPs) with varying amounts of *T. parthenium* extract after 30 min. (A, B, and C indicate 5, 10, and 20 mL of Feverfew extract with 95,90, and 80 mL of 0.001 M silver nitrate aqueous solution, respectively).

To evaluate the effect of time on the peaks generated by sample C, UV–vis spectra were recorded at six intervals over a 24 h period. As shown in Figure 3, the spectra ranged from 360 to 440 nm, with a prominent SPR band at 400 nm. The broadening of the peaks indicates uniform nanoparticle size. AgNP formation began after 30 min and increased significantly up to 24 h. No further color change was observed beyond 24 h, suggesting the completion of the nanoparticle synthesis process.

The synthesis of AgNPs started approximately 10 min after the combination mixing the feverfew extracts with the silver nitrate solution, showing significant enhancement until 24 h. Beyond this timeframe, while the mixture was still on the shaker, no alteration occurred in color, suggesting the finalization of the nanoparticle synthesis process.

Zeta potential measurement shape

The zeta potential measurement of AgNPs reveals insights into their stability and surface charge. Biogenic AgNPs exhibit lower zeta potential values in smaller extract quantities and higher values in larger quantities. Sample C displayed a zeta potential range of -30 to -90 mV, indicating enhanced stability of the AgNPs (Fig. 4).

DLS analysis

Dynamic Light Scattering (DLS) is a widely used technique for measuring particle size distribution in solution. By analyzing variations in light scattering

intensity caused by the Brownian motion of particles, DLS provides valuable information about their size and distribution. Figure 5 shows the particle size distribution (PSD) of bioinspired AgNPs measured using a Zetasizer (Malvern). The PSD ranged from 64 to 82 nm, with an average particle size of 68.6 nm.

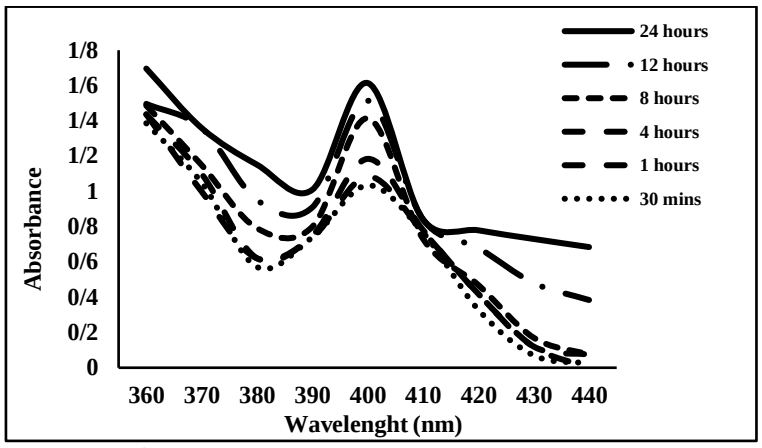

Fig. 3. The absorbance spectrum of silver nanoparticles (AgNPs) synthesized by *T. parthenium* extract at time intervals.

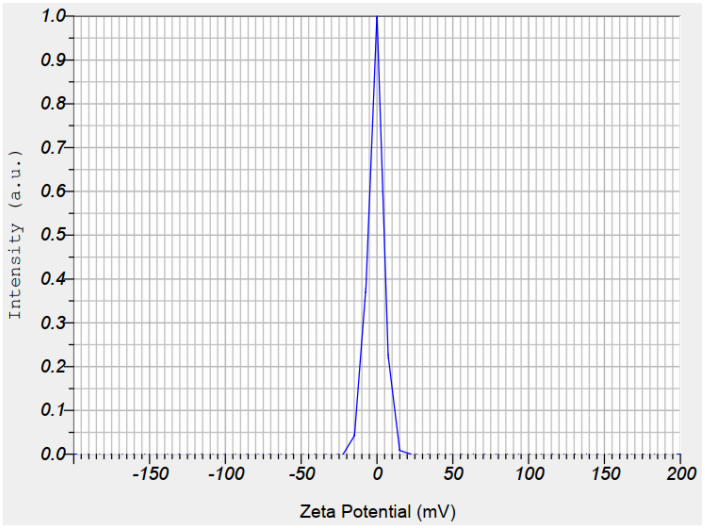

Fig. 4. Zeta potential analysis of silver nanoparticles (AgNPs) synthesized by *T. parthenium* extract.

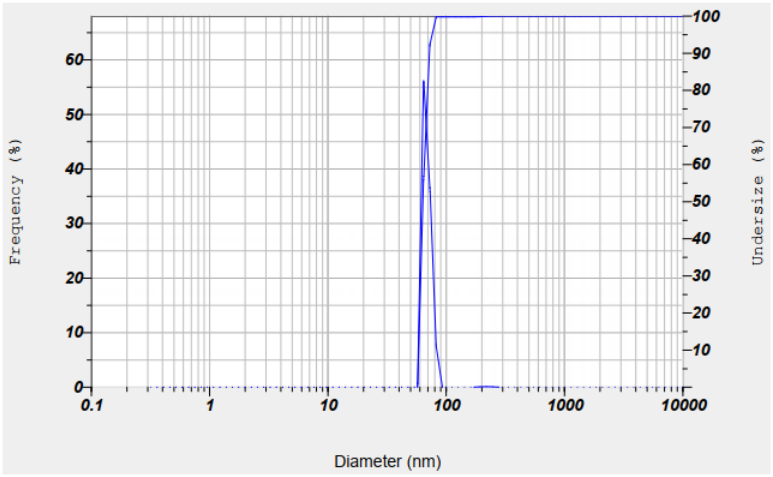

Fig. 5. Dynamic light scattering (DLS) spectrum of silver nanoparticles (AgNPs) synthesized using *T. parthenium* extract.

FESEM and EDX analysis

After successfully synthesizing AgNPs, FESEM analysis was carried out (Fig. 6a). The image revealed the formation of nearly spherical nanoparticles with an average size of 65.7 nm. The particles were uniformly dispersed and consistent in size, demonstrating the effectiveness of the feverfew extract in the synthesis process. FESEM results suggest that the reducing agents present in plant-mediated synthesis play a key role in nanoparticle formation. Using medicinal plants for AgNP synthesis not only enables control over particle size and shape but also imparts antimicrobial properties from the plants to the nanoparticles.

For EDX analysis, the AgNPs were dried and drop-coated onto a carbon film. The analysis was performed using a thermal energy X-ray analyzer (EDX) coupled with FESEM. The resulting EDX spectrum of AgNPs synthesized from feverfew extract is shown in Figure 6b. The tallest peak corresponds to silver, confirming the presence of AgNPs in the sample.

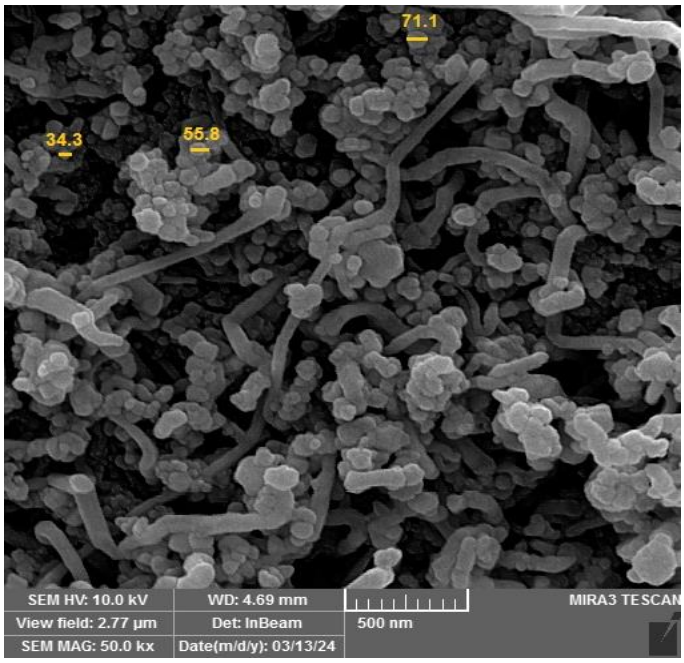

a

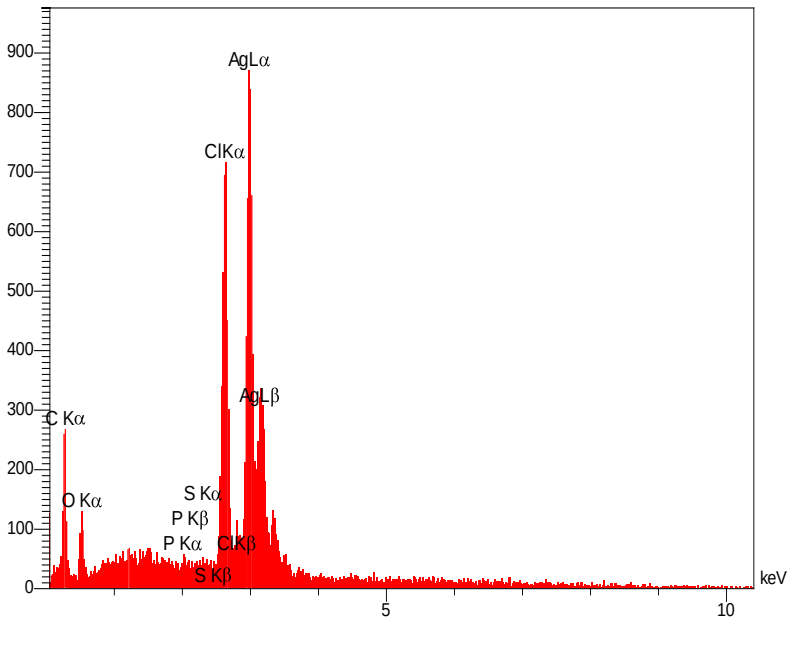

b

Fig. 6. (**a**) Field emission scanning electron microscopy (FESEM) images and (**b**) energy dispersive X-ray (EDX) analysis of biosynthesized silver nanoparticles (AgNPs) produced using *T. parthenium* extract.

XRD analysis

The AgNPs structure and crystalline size were analyzed via XRD. Figure 7 shows a typical XRD pattern of the AgNPs synthesized using *T. parthenium* extract after conversion of Ag^{+} cations to Ag^{o}. Four diffraction peaks at 2θ values of 38.05, 44.12, 67.48, and 77.15° correspond to the planes (111), (200), (220), and (311), respectively. The crystalline size of AgNPs was determined using Debye-Scherrer's formula employed in XRD analysis to estimate the average grain size of the crystallite in the material. It connects the grain size (D) to the X-ray wavelength (λ) and the diffraction peak full width at half maximum (β). The equation is expressed as:

$$D = \frac{K\lambda}{(\beta\ cos\theta)} \quad (1)$$

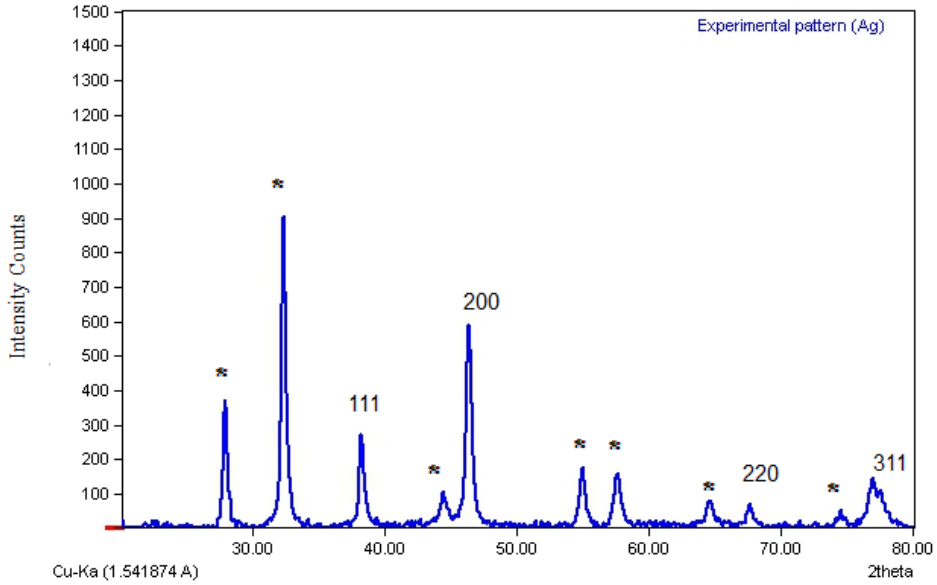

Fig. 7. X-ray diffraction (XRD) profiles of silver nanoparticles (AgNPs) at different quantities of *T. parthenium* extract. The additional peaks indicated with * may be due to the bio-inorganic compounds and proteins present in the extract.

Where K is a dimensionless shape factor usually close to 0.9. This equation offers a straightforward yet useful method for researchers to ascertain the size of crystalline domains in a material using XRD data (Cullity, 1956). The average diameter of the synthesized nanoparticles was determined by XRD line expanding, which was approximately well aligned with those acquired from FESEM and DLS. From XRD, DLS and FESEM, the average sizes of particles were determined to be almost 67.7, 68.6, and 65.7 nm, respectively.

FTIR spectrum analysis

FTIR spectroscopy is useful for analyzing the potential interactions of AgNPs with different functional groups. Figure 8 displays the FTIR spectra of *T. perthenium* extract alongside bio-reduced AgNPs that reveals reveal the different functional groups groups' presence at different positions. The synthesized AgNPs solution contained numerous molecules, which some molecules adsorbed on the surface of AgNPs (Tripathy et al., 2010). Several prominent absorbance bands were detected at approximately 3207, 1515, 1245, 1123, 1082, 792, 595, and 534 cm^{-1}. The peaks for AgNPs were detected at 3436, 2929, 1604, 1383, and 1029 cm^{-1}. The peaks observed in the spectrum suggest the presence of functional groups associated with the AgNPs. The peak at 3436 cm^{-1} suggested the presence of O-H stretching vibration, while the peak at 2929 cm^{-1} correlated with to C-H stretching vibrations.

Discussion

Plant-mediated synthesis offers a sustainable approach for producing AgNPs, as plant materials are readily available, environmentally friendly, renewable, and cost-effective (Hamouda et al., 2019; Aboyewa et al., 2021b). Phytochemicals present in plant extracts—derived from roots, stems, and leaves—play a vital role in this process (Karmous et al., 2020). These extracts are rich in molecules containing functional groups such as carboxyl, amino, carbonyl, hydroxyl, and phenol, which enable the reduction of metals like silver (Rafique et al., 2017), gold (Aboyewa et al., 2021a), and platinum (Fahmy et al., 2020). Antioxidants act as both reducing and capping agents, with flavonoids (e.g., flavonols, flavan-3-ols), phenolic acids (e.g., benzoic, hydroxycinnamic, and ellagic acids) (Khodadadi et al., 2017), and anthocyanins (Simon et al., 2021) playing particularly important roles.

In many cases, a color shift to brown or yellow indicates AgNP formation, corresponding to the surface plasmon resonance (SPR) of silver nanoparticles (Shankar et al., 2004b). The brown coloration arises from free electron oscillation (Mulvaney, 1996). While phytochemicals are primarily responsible for the bioreduction of metal cations, other plant metabolites, including proteins and chlorophyll, contribute to nanoparticle stabilization (Srikar et al., 2016). Key phytochemicals involved in reduction include aldehydes, ketones, flavones, sugars, terpenoids, carboxylic acids, and amides (Singh et al., 2018).

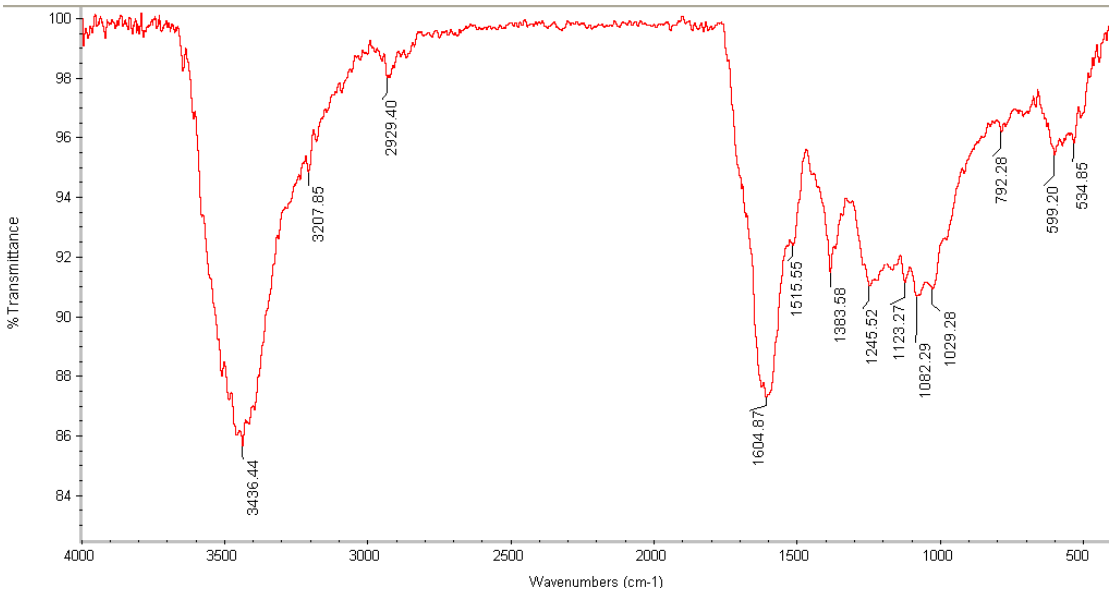

Fig. 8. Fourier transform infrared spectroscopy (FTIR) spectrum of synthesized silver nanoparticles (AgNPs) by *T. parthenium* extract.

UV–Vis spectroscopy is commonly used to confirm AgNP formation (Nanda and Saravanan, 2009). Studies show that increasing extract concentration often produces smaller particle sizes, consistent with previous reports (Aromal and Philip, 2012; Zayed and Eisa, 2014). In the present work, UV–Vis spectra exhibited a distinct SPR band at 400 nm, confirming AgNP synthesis, which aligns with earlier findings in the 350–450 nm range (Ashokkumar et al., 2014). The absence of further color change after 24 h indicated completion of the synthesis process, consistent with reports on *Lippia citriodora*, where AgNPs formed within 24 h also displayed bound plant compounds and functional groups (Cruz et al., 2010; Ebadi et al., 2017).

The synthesized AgNPs demonstrated strong stability, with zeta potential values ranging from –30 to –90 mV. Values between –40 and –50 mV indicate good stability (Salopek et al., 1992), while more negative values suggest increased interparticle repulsion and reduced aggregation, further enhancing nanoparticle stability (Kotakadi et al., 2013). The average particle size of 68.6 nm also supports the stability of the synthesized AgNPs (Patil et al., 2012), a value that reflects the hydrodynamic sizes typical of nanomaterials (Gurunathan et al., 2009).

Recently, applications have expanded to include the characterization of various nanomaterials and their properties (Das et al., 2014). The working principle of X-ray diffraction is based on Bragg's law (Waseda et al., 2011). The broadening of Bragg's peaks indicates the nanoscale dimensions of the particles, confirming nanoparticle formation. As mentioned earlier, diffraction peaks for AgNPs were observed at 2θ values of 38.05, 44.12, 67.48, and 77.15º. Additionally, reports indicated that AgNPs are crystalline in nature and exhibit a face-centered cubic (FCC) structure (Kharat and Mendhulkar, 2016; Ren et al., 2019). This XRD pattern provides valuable insights into the structural properties of the synthesized AgNPs, highlighting their potential for various applications in nanotechnology and related fields (Temgire and Joshi, 2004). FESEM imaging revealed synthesized AgNPs with an average size of 65.7 nm, consistent with hydrodynamic sizes reported in other research cases (Gurunathan et al., 2009). These results suggest potential nano-medicine applications for biocompatible, biologically active nanoparticles (Tippayawat et al., 2016). The EDX spectrum of AgNPs exhibited a strong silver signal, as confirmed by an emission peak around 3 keV, indicating silver as the primary component (Sathishkumar et al., 2009). XRD analysis had revealed crystalline silver nanoparticles, with peaks at 38.05, 44.12, 67.48, and 77.15º, consistent with Anuradha et al. (2010). This aligns well with the expected nanoscale dimensions. (Anuradha, 2010).

FTIR spectra of bio-reduced AgNPs revealed peaks at 1604 cm^{-1} (C=C stretching), 1383 cm^{-1} (C-N stretching), and 1029 cm^{-1} (C-O stretching) (Khalil et al., 2012), indicating the presence of amide (I) groups, aromatic amines, secondary alcohols, and phenolic groups. These functional groups likely acted as reducing agents during AgNP synthesis. Furthermore, phytochemicals appear to stabilize the nanoparticles by preventing aggregation, contributing to long-term stability (Borchert et al., 2005).

Conclusion

In the present study, silver nanoparticles (AgNPs) were successfully synthesized using an aqueous extract of *Tanacetum parthenium* (leaf and flower). The method proved to be efficient, cost-effective, rapid, and environmentally friendly. Characterization studies confirmed the successful formation of nanoparticles with a narrow size distribution and good stability. Comprehensive analyses of nanoparticle structure, morphology, and size using zeta potential, DLS, FESEM, EDX, and XRD, along with chemical composition studies via FT-IR and UV–Vis spectroscopy, confirmed the presence of AgNPs. FT-IR and FESEM results further suggested that flavonoids and proteins in the extract formed a protective coating on the AgNPs, aiding in their stabilization and preventing agglomeration. These findings highlight the potential of *T. parthenium* extract as a sustainable green synthesis route for nanoparticle production. The presence of diverse functional groups in the plant extract contributes to both nanoparticle formation and stability. Importantly, this approach provides a safe and eco-friendly alternative to conventional methods that often rely on hazardous materials. In conclusion, phytosynthesis of metal nanoparticles such as AgNPs offers a convenient, scalable, low-cost, and environmentally friendly process compared to traditional synthesis methods. The successful use of *T. parthenium* extract not only demonstrates the feasibility of sustainable nanomaterial production but also opens new opportunities for applications in medicine, agriculture, and environmental remediation. With its efficiency, scalability, and cost-effectiveness, this method presents a promising pathway for the large-scale production of diverse nanomaterials.

Acknowledgments

This article resulted from a PhD dissertation approved by the Vice-Chancellery for Research and Technology at Ferdowsi University of Mashhad (code: 53936).

Author Contributions

SS and MA contributed to conceptualization; SS performed methodology, software, formal analysis, investigation, resources, data curation, project administration, and writing—original draft preparation; SS and M carried out validation; MA and NM contributed to writing—review and editing; MA was responsible for visualization and funding acquisition; and NM supervised the study. All authors have read and approved the final manuscript.

Funding

This research was supported financially by Ferdowsi University of Mashhad under grant number 53936.

Conflict of Interest

The authors indicate no conflict of interest in this work.

Reference

Aboyewa JA, Sibuyi NR, Meyer M, Oguntibeju OO. 2021a. Gold nanoparticles synthesized using extracts of cyclopia intermedia, commonly known as honeybush, amplify the cytotoxic effects of doxorubicin. Nanomaterials 11, 132.

Aboyewa JA, Sibuyi NR, Meyer M, Oguntibeju OO. 2021b. Green synthesis of metallic nanoparticles using some selected medicinal plants from southern africa and their biological applications. Plants 10, 1929.

Alqudami A, Annapoorni S. 2007. Fluorescence from metallic silver and iron nanoparticles prepared by exploding wire technique. Plasmonics 2, 5-13.

Anuradha TV. 2010. Mesolamellar composite of TiN and CTAB using fluoride ion bridge: synthesis, mechanism & characterization. Natural Science 2, 464-468.

Araghi AM, Nemati H, Azizi M, Moshtaghi N, Shoor M, Hadian J. 2019. Assessment of phytochemical and agro-morphological variability among different wild accessions of *Mentha longifolia* L. cultivated in field condition. Industrial Crops and Products 140, 111698.

Aromal SA, Philip D. 2012. Green synthesis of gold nanoparticles using *Trigonella foenum-graecum* and its size-dependent catalytic activity. Spectrochimica Acta Part A: Molecular and Biomolecular Spectroscopy 97, 1-5.

Ashokkumar S, Ravi S, Kathiravan V, Velmurugan S. 2014. RETRACTED: Synthesis, characterization and catalytic activity of silver nanoparticles using Tribulus terrestris leaf extract. Elsevier.

Ashour AA, Raafat D, El-Gowelli HM, El-Kamel AH. 2015. Green synthesis of silver nanoparticles using cranberry powder aqueous extract: characterization and antimicrobial properties. International Journal of Nanomedicine, 7207-7221.

Aziz M, Kaboli Farshch H, Oroojalian F, Orafaee H. 2018. Green Synthesis of Silver Nano-particles Using Kelussia odoratissima Mozaff. Extract and Evaluation of its Antibacterial Activity.

Balashanmugam P. 2015. Assessment of Toxicity and Prospective Wound Healing Properties of Phytosynthesized Silver and Gold Nanoparticles from Cassia Roxburghii DC (PhD Thesis). University of Madras, Chennai, India.

Baruwati B, Polshettiwar V, Varma RSJGc. 2009. Glutathione promoted expeditious green synthesis of silver nanoparticles in water using microwaves. 11, 926-930.

Bhumkar DR, Joshi HM, Sastry M, Pokharkar VB. 2007. Chitosan reduced gold nanoparticles as novel carriers for transmucosal delivery of insulin. Pharmaceutical research 24, 1415-1426.

Borchert H, Shevchenko EV, Robert A, Mekis I, Kornowski A, Grübel G, Weller H. 2005. Determination of nanocrystal sizes: a comparison of TEM, SAXS, and XRD studies of highly monodisperse CoPt3 particles. Langmuir 21, 1931-1936.

Chandran SP, Chaudhary M, Pasricha R, Ahmad A, Sastry M. 2006. Synthesis of gold nanotriangles and silver nanoparticles using *Aloe vera* plant extract. Biotechnology Progress 22, 577-583.

Cruz D, Falé PL, Mourato A, Vaz PD, Serralheiro ML, Lino ARL. 2010. Preparation and physicochemical characterization of Ag nanoparticles biosynthesized by *Lippia citriodora* (Lemon verbena). Colloids and surfaces B: Biointerfaces 81, 67-73.

Cui Y, Lieber CM. 2001. Functional nanoscale electronic devices assembled using silicon nanowire building blocks. Science 291, 851-853.

Cullity BD. 1956. Elements of X-ray Diffraction: Addison-Wesley Publishing.

Das S, Roy P, Pal R, Auddy RG, Chakraborti AS, Mukherjee A. 2014. Engineered silybin nanoparticles educe efficient control in experimental diabetes. PLoS One 9, e101818.

Dobelis IN. 1986. Magic and medicine of plants. Pleasantville, NY: Reader's Digest Association, p. 702.

Dubey SP, Lahtinen M, Särkkä H, Sillanpää M. 2010. Bioprospective of Sorbus aucuparia leaf extract in development of silver and gold nanocolloids. Colloids and Surfaces B. Biointerfaces 80, 26-33.

Ebadi MT, Sefidkon F, Azizi M, Ahmadi N. 2017. Packaging methods and storage duration affect essential oil content and composition of lemon verbena (*Lippia citriodora* Kunth.). Food Science & Nutrition 5, 588-595.

El-Sayed MA. 2001. Some interesting properties of metals confined in time and nanometer space of different shapes. Accounts of chemical research 34, 257-264.

Elumalai E, Prasad T, Hemachandran J, Therasa SV, Thirumalai T, David E. 2010. Extracellular synthesis of silver nanoparticles using leaves of *Euphorbia hirta* and their antibacterial activities. Journal of Pharmacology Science Research 2, 549-554.

Fahmy SA, Preis E, Bakowsky U, Azzazy HME-S. 2020. Platinum nanoparticles: green synthesis and biomedical applications. Molecules 25, 4981.

Farshchi HK, Azizi M, Jaafari MR, Nemati SH, Fotovat A. 2018. Green synthesis of iron nanoparticles by Rosemary extract and cytotoxicity effect evaluation on cancer cell lines. Biocatalysis and Agricultural Biotechnology 16, 54-62.

Gurunathan S, Kalishwaralal K, Vaidyanathan R, Venkataraman D, Pandian SRK, Muniyandi J, Hariharan N, Eom SH. 2009. Biosynthesis, purification and characterization of silver nanoparticles using *Escherichia coli*. Colloids and surfaces B. Biointerfaces 74, 328-335.

Hamouda RA, Hussein MH, Abo-Elmagd RA, Bawazir SS. 2019. Synthesis and biological characterization of silver nanoparticles derived from the cyanobacterium *Oscillatoria limnetica*. Scientific reports 9, 13071.

He L, Gao S-y, Wu H, Liao X-p, He Q, Shi B. 2012. Antibacterial activity of silver nanoparticles stabilized on tannin-grafted collagen fiber. Materials Science and Engineering: C 32, 1050-1056.

Heptinstall S, Awang D, Dawson B, Kindack D, Knight D, May J. 1992. Parthenolide content and bioactivity of feverfew (*Tanacetum parthenium* (L.) Schultz-Bip.). Estimation of commercial and authenticated feverfew products. Journal of pharmacy and pharmacology 44, 391-395.

Hoag GE, Collins JB, Holcomb JL, Hoag JR, Nadagouda MN, Varma RSJJoMC. 2009. Degradation of bromothymol blue by 'greener'nano-scale zero-valent iron synthesized using tea polyphenols. 19, 8671-8677.

Horwat D, Zakharov D, Endrino J, Soldera F, Anders A, Migot S, Karoum R, Vernoux P, Pierson JJS, Technology C. 2011. Chemistry, phase formation, and catalytic activity of thin palladium-containing oxide films synthesized by plasma-assisted physical vapor deposition. 205, S171-S177.

Huang J, Li Q, Sun D, Lu Y, Su Y, Yang X, Wang

H, Wang Y, Shao W, He N. 2007. Biosynthesis of silver and gold nanoparticles by novel sundried Cinnamomum camphora leaf. Nanotechnology 18, 105104.

Kalishwaralal K, Deepak V, Pandian SRK, Kottaisamy M, BarathManiKanth S, Kartikeyan B, Gurunathan S. 2010. Biosynthesis of silver and gold nanoparticles using Brevibacterium casei. Colloids and Surfaces B: Biointerfaces 77, 257-262.

Karmous I, Pandey A, Haj KB, Chaoui A. 2020. Efficiency of the green synthesized nanoparticles as new tools in cancer therapy: insights on plant-based bioengineered nanoparticles, biophysical properties, and anticancer roles. Biological Trace Element Research 196, 330-342.

Kaviya S, Santhanalakshmi J, Viswanathan B, Muthumary J, Srinivasan K. 2011. Biosynthesis of silver nanoparticles using *Citrus sinensis* peel extract and its antibacterial activity. Spectrochimica Acta Part A: Molecular and Biomolecular Spectroscopy 79, 594-598.

Khalil MM, Ismail EH, El-Magdoub F. 2012. Biosynthesis of Au nanoparticles using olive leaf extract: 1st nano updates. Arabian Journal of Chemistry 5, 431-437.

Khan Y, Sadia H, Ali Shah SZ, Khan MN, Shah AA, Ullah N, Ullah MF, Bibi H, Bafakeeh OT, Khedher NB. 2022. Classification, synthetic, and characterization approaches to nanoparticles, and their applications in various fields of nanotechnology: A review. Catalysts 12, 1386.

Kharat SN, Mendhulkar VD. 2016. Synthesis, characterization and studies on antioxidant activity of silver nanoparticles using *Elephantopus scaber* leaf extract. Materials Science and Engineering C 62, 719-724.

Khodadadi B, Bordbar M, Yeganeh-Faal A, Nasrollahzadeh M. 2017. Green synthesis of Ag nanoparticles/clinoptilolite using *Vaccinium macrocarpon* fruit extract and its excellent catalytic activity for reduction of organic dyes. Journal of Alloys and Compounds 719, 82-88.

Kotakadi VS, Rao YS, Gaddam SA, Prasad T, Reddy AV, Gopal DS. 2013. Simple and rapid biosynthesis of stable silver nanoparticles using dried leaves of *Catharanthus roseus*. Linn. G. Donn and its anti microbial activity. Colloids and Surfaces B: Biointerfaces 105, 194-198.

Kouvaris P, Delimitis A, Zaspalis V, Papadopoulos D, Tsipas SA, Michailidis N. 2012. Green synthesis and characterization of silver nanoparticles produced using Arbutus Unedo leaf extract. Materials Letters 76, 18-20.

Kumar V, Yadav SK. 2009. Plant-mediated synthesis of silver and gold nanoparticles and their applications. Journal of Chemical Technology & Biotechnology: International Research in Process, Environmental & Clean Technology 84, 151-157.

Mulvaney P. 1996. Surface plasmon spectroscopy of nanosized metal particles. Langmuir 12, 788-800.

Nanda A, Saravanan M. 2009. Biosynthesis of silver nanoparticles from *Staphylococcus aureus* and its antimicrobial activity against MRSA and MRSE. Nanomedicine: Nanotechnology, Biology and Medicine 5, 452-456.

Narayanan KB, Sakthivel N. 2010. Biological synthesis of metal nanoparticles by microbes. Advances in Colloid and Interface Science 156, 1-13.

Patil SV, Borase HP, Patil CD, Salunke BK. 2012. Biosynthesis of silver nanoparticles using latex from few euphorbian plants and their antimicrobial potential. Applied Biochemistry and Biotechnology 167, 776-790.

Rafique M, Sadaf I, Rafique MS, Tahir MB. 2017. A review on green synthesis of silver nanoparticles and their applications. Artificial Cells, Nanomedicine, and Biotechnology 45, 1272-1291.

Rajesh W, Jaya R, Niranjan S, Vijay D, Sahebrao B. 2009. Phytosynthesis of Silver Nanoparticle Using *Gliricidia sepium* (Jacq.). Current Nanoscience 5, 117–122.

Ren Y-y, Yang H, Wang T, Wang C. 2019. Bio-synthesis of silver nanoparticles with antibacterial activity. Materials Chemistry and Physics 235, 121746.

Salopek B, Krasic D, Filipovic S. 1992. Measurement and application of zeta-potential. Rudarsko-geolosko-naftni zbornik 4, 147.

Samadi S, Saharkhiz MJ, Azizi M, Samiei L, Karami A, Ghorbanpour M. 2021. Single-wall carbon nano tubes (SWCNTs) penetrate *Thymus daenensis* Celak. plant cells and increase secondary metabolite accumulation in vitro. Industrial Crops and Products 165, 113424.

Sathishkumar M, Sneha K, Won S, Cho C-W, Kim S, Yun Y-S. 2009. *Cinnamon zeylanicum* bark extract and powder mediated green synthesis of nano-crystalline silver particles and its bactericidal activity. Colloids and Surfaces B: Biointerfaces 73, 332-338.

Sathyavathi R, Krishna M, Rao S, Saritha R, Rao D. 2010. Silver has the advantage of having broad antimicrobial biosynthesis of silver nanoparticles using *Coriandrum sativum* leaf extract activities against gram-negative and gram-positive bacteria

and their application in nonlinear optics. Advances in Scientific Letters 3, 1-6.

Schneidewind H, Schüler T, Strelau KK, Weber K, Cialla D, Diegel M, Mattheis R, Berger A, Möller R, Popp J. 2012. The morphology of silver nanoparticles prepared by enzyme-induced reduction. Beilstein Journal of Nanotechnology 3, 404-414.

Shahhoseini R, Azizi M, Asili J, Moshtaghi N, Samiei L. 2020. Effects of zinc oxide nanoelicitors on yield, secondary metabolites, zinc and iron absorption of Feverfew (*Tanacetum parthenium* (L.) Schultz Bip.). Acta Physiologiae Plantarum 42, 1-18.

Shankar SS, Ahmad A, Sastry M. 2003. Geranium leaf assisted biosynthesis of silver nanoparticles. Biotechnology Progress 19, 1627-1631.

Shankar SS, Rai A, Ahmad A, Sastry M. 2004a. Rapid synthesis of Au, Ag, and bimetallic Au core–Ag shell nanoparticles using Neem (*Azadirachta indica*) leaf broth. Journal of Colloid and Interface Science 275, 496-502.

Shankar SS, Rai A, Ankamwar B, Singh A, Ahmad A, Sastry M. 2004b. Biological synthesis of triangular gold nanoprisms. Nature Materials 3, 482-488.

Simon S, Sibuyi NRS, Fadaka AO, Meyer M, Madiehe AM, du Preez MG. 2021. The antimicrobial activity of biogenic silver nanoparticles synthesized from extracts of red and green European pear cultivars. Artificial Cells, Nanomedicine, and Biotechnology 49, 613-624.

Singh P, Ahn S, Kang J-P, Veronika S, Huo Y, Singh H, Chokkaligam M, El-Agamy Farh M, Aceituno VC, Kim YJ. 2018. In vitro anti-inflammatory activity of spherical silver nanoparticles and monodisperse hexagonal gold nanoparticles by fruit extract of *Prunus serrulata*: a green synthetic approach. Artificial Cells, Nanomedicine, and Biotechnology 46, 2022-2032.

Sondi I, Salopek-Sondi B. 2004. Silver nanoparticles as antimicrobial agent: a case study on *E. coli* as a model for Gram-negative bacteria. Journal of Colloid and Interface Science 275, 177-182.

Song JY, Jang H-K, Kim BS. 2009a. Biological synthesis of gold nanoparticles using *Magnolia kobus* and Diopyros kaki leaf extracts. Process Biochemistry 44, 1133-1138.

Song JY, Kim BSJB, engineering b. 2009b. Rapid biological synthesis of silver nanoparticles using plant leaf extracts 32, 79-84.

Srikanth H, Hajndl R, Chirinos C, Sanders J, Sampath A, Sudarshan T. 2001. Magnetic studies of polymer-coated Fe nanoparticles synthesized by microwave plasma polymerization. Applied Physics Letters 79, 3503-3505.

Srikar SK, Giri DD, Pal DB, Mishra PK, Upadhyay SN. 2016. Green synthesis of silver nanoparticles: a review. Green and Sustainable Chemistry 6, 34.

Sulaiman GM, Mohammed WH, Marzoog TR, Al-Amiery AAA, Kadhum AAH, Mohamad AB. 2013. Green synthesis, antimicrobial and cytotoxic effects of silver nanoparticles using Eucalyptus chapmaniana leaves extract. Asian Pacific Journal of Tropical Biomedicine 3, 58-63.

Sun Y, Mayers B, Herricks T, Xia Y. 2003. Polyol synthesis of uniform silver nanowires: a plausible growth mechanism and the supporting evidence. Nano Letters 3, 955-960.

Temgire M, Joshi S. 2004. Optical and structural studies of silver nanoparticles. Radiation Physics and Chemistry 71, 1039-1044.

Tippayawat P, Phromviyo N, Boueroy P, Chompoosor A. 2016. Green synthesis of silver nanoparticles in aloe vera plant extract prepared by a hydrothermal method and their synergistic antibacterial activity. PeerJ 4, e2589.

Tripathy A, Raichur AM, Chandrasekaran N, Prathna T, Mukherjee A. 2010. Process variables in biomimetic synthesis of silver nanoparticles by aqueous extract of *Azadirachta indica* (Neem) leaves. Journal of Nanoparticle Research 12, 237-246.

Tuutijärvi T, Lu J, Sillanpää M, Chen G. 2009. As (V) adsorption on maghemite nanoparticles. Journal of Hazardous Materials 166, 1415-1420.

Valle-Orta M, Diaz D, Santiago-Jacinto P, Vázquez-Olmos A, Reguera E. 2008. Instantaneous synthesis of stable zerovalent metal nanoparticles under standard reaction conditions. The Journal of Physical Chemistry B 112, 14427-14434.

Vilchis-Nestor AR, Sánchez-Mendieta V, Camacho-López MA, Gómez-Espinosa RM, Camacho-López MA, Arenas-Alatorre JA. 2008. Solventless synthesis and optical properties of Au and Ag nanoparticles using *Camellia sinensis* extract. Materials Letters 62, 3103-3105.

Vimalanathan A, Vishakha Tyagi VT, Rajesh A, Preethi Devanand PD, Tyagi M. 2013. Biosynthesis of silver nanoparticles using Chinese white ginseng plant root Panax ginseng.

Waseda Y, Matsubara E, Shinoda K. 2011. X-ray diffraction crystallography: introduction, examples and solved problems: Springer Science & Business Media.

Yang X, Li Q, Wang H, Huang J, Lin L, Wang W,

Sun D, Su Y, Opiyo JB, Hong L. 2010. Green synthesis of palladium nanoparticles using broth of Cinnamomum camphora leaf. Journal of Nanoparticle Research 12, 1589-1598.

Yaqoob AA, Umar K, Ibrahim MNM. 2020. Silver nanoparticles: various methods of synthesis, size affecting factors and their potential applications–a review. Applied Nanoscience 10, 1369-1378.

Zayed MF, Eisa WH. 2014. Phoenix dactylifera L. leaf extract phytosynthesized gold nanoparticles; controlled synthesis and catalytic activity. Spectrochimica Acta Part A: Molecular and Biomolecular Spectroscopy 121, 238-244.

Zhang H-w, Liu Y, Sun S-h. 2010. Synthesis and assembly of magnetic nanoparticles for information and energy storage applications. Frontiers of Physics in China 5, 347-356.